Marine Geology 260 (2009) 81–89

Contents lists available at ScienceDirect

Marine Geology

journal homepage: www.elsevier.com/locate/margeo

Deposits related to the failure of the Malpasset Dam in 1959 An analogue for hyperpycnal deposits from jökulhlaups

T. Mulder [a,*], S. Zaragosi [a], J.-M. Jouanneau [a], G. Bellaiche [b], S. Guérinaud [a], J. Querneau [a]

[a] Université de bordeaux, UMR 5805 EPOC, avenue des facultés, F-33405 Talence cedex
[b] Hameau de la Corne d'Or, 12 Boulevard Corne d'Or, 06230 Villefranche-sur-Mer, France

ARTICLE INFO

Article history:
Received 25 July 2008
Received in revised form 3 February 2009
Accepted 4 February 2009

Keywords:
flood
freezing
inertia flow
jökulhlaup
Malpasset Dam break
surge-flow
SE France

ABSTRACT

Sediment cores collected in the Gulf of Fréjus (SE France) contain submarine deposits related to the failure of the Malpasset Dam in 1959. These deposits constitute a dark, sandy terrigeneous layer of 10–40 cm thickness lying above an erosion surface. The deposits are composed of ungraded, non-bioturbated sands and silts displaying no apparent sedimentary structure, but rich in organic matter and rock or shell fragments. During the event, this layer prograded onto the inner continental shelf and froze rapidly. These hyperconcentrated flow deposits are related to an unsteady inertia flow generated by a surge-like flood and bedload-dominated hyperpycnal flow. Rapid freezing on flow sides generated lateral, coarse-grained, levee-shape deposits. The deposits related to the failure of the Malpasset Dam are drastically different from classical suspended-load-dominated hyperpycnites deposited by a steady, flood-generated, hyperpycnal flow. However, they are comparable with present-day deposits on a volcanic, ice-covered margin (Icelandic jökulhlaups), with ancient deposits resulting from the pulsating output of subglacial lakes during a deglaciation, or with Martian landforms resulting from sporadic ice–melt events during early Martian times.

1. Introduction

Submarine turbidity currents can have two main origins (Normark and Piper, 1991). They can result from the transformation of a submarine slide into an initially laminar and then turbulent flow. They can also result from the direct transformation of a river flow entering the sea during a flood, when the suspended sediment concentration is high enough to form a non-buoyant plume (hyperpycnal flows of Bates, 1953; Mulder and Syvitski, 1995; Nakajima, 2006). In this latter case, the flow becomes a turbidity current and its velocity reflects variations of the flood hydrograph at the river mouth. These variations are recorded in hyperpycnal deposits (hyperpycnites of Mulder et al., 2002) that show a coarsening-up interval deposited during the period of increasing discharge and a fining-up-interval deposited during the period of decreasing discharge. Hyperpycnal flows with high suspended sediment load occur preferentially at the mouths of small mountain rivers (Milliman and Syvitski, 1992), and the duration of the floods depends on the climatic environment (Wright et al., 1986; Mulder et al., 1998a,b; Saint-Onge et al., 2003; Warrick and Milliman, 2003; Milliman and Kao 2005; Yu, 2006). For high-magnitude floods, the basal unit can be eroded during peak flood conditions generating a hyperpycnite with missing base resembling a classical Bouma sequence (Bouma, 1962; Mulder et al., 2001b; Mulder et al., 2002).

Catastrophic events can also produce hyperpycnal flows but, in this case, bedload transport is dominant. For example, the sudden emptying of a subglacial reservoir filled by meltwater during the eruption of the Grimsvötn volcano (Iceland) in 1996 produced a Jökulhlaup that reached 50 000 $m^3\ s^{-1}$ on the Skeidararsandur (Grönvold and Jóhannesson, 1984; Einarsson et al., 1997; Gudmunsson et al., 1997). A total water volume of 3 km^3 discharged into the ocean in only two days, with sediment concentration reaching reached 200 kg/m^3 (Mulder et al., 2003). Similar triggering can occur at a higher magnitude during the deglaciation of a major ice-sheet. Brunner et al. (1999) and Zuffa et al. (2000) described deposits related to hyperpycnal outburst of glacial Lake Missoula (Utah) during late Pleistocene (17–12 ka). The 2000 km^3 lake drained 40 to 80 times generating multiple floods with estimated peak discharges of about $10^7\ m^3\ s^{-1}$ (Mulineaux et al., 1978; Baker and Bunker, 1985; Waitt, 1985). The related deposits were cored during an IODP leg (Shipboard Scientific Party, 1998a,b,c; Brunner et al., 1999; Zierenberg et al., 2000). They show several metre-thick massive, crudely-graded, sand beds corresponding to hyperconcentrated and concentrated flow deposits (Mulder and Alexander, 2001). The contemporaneous emptying of Lake Bonneville in Oregon (estimated volume, 1583 km^3; Gilbert, 1878; Malde, 1968) produced a flood with an estimated peak discharge of $425 \times 10^3\ m^3\ s^{-1}$ (Richmond et al., 1965) and transported large basalt boulders of several metres diameter (Malde and Powers, 1962). Dromart et al. (2007) reported steeply-inclined clinoforms in Valles Marineris that could be related to outburst flow occurring during

* Corresponding author.
E-mail address: t.mulder@epoc.u-bordeaux1.fr (T. Mulder).

0025-3227/$ – see front matter © 2009 Elsevier B.V. All rights reserved.
doi:10.1016/j.margeo.2009.02.002

Hesperian times (3.5 Ga) when Martian atmospheric pressure was high enough to temporarily allow ice-melting.

In this paper, we use the catastrophic flood event resulting from the failure of the Malpasset Dam as an analogue for bedload-dominated hyperpycnal flows generated by sudden flash floods occurring during natural dam breakage or similar outburst events to describe the nature and distribution of the resulting marine deposits and to interpret the associated transport and deposition processes.

2. Regional setting

The study area is located in the western Mediterranean basin (Fig. 1) at the southern geological limit of Calcareous Provence where massive Cretaceous carbonates outcrop. The study area also includes a part of the Tanneron and Esterel massifs (Fig. 2A). The Tanneron is a Hercynian massif containing granites, gneiss and coal deposits and the Esterel is formed by Permian volcanic deposits. The eastern part of the study area is occupied by a Permian depression that forms the western end of the Esterel Massif and shows sedimentary and volcanic Permian deposits.

The combined Argens and Reyran rivers discharge into the Gulf of Fréjus, which is approximately 4 km wide (Fig. 1). Both rivers originate in the Calcareous Provence; the Reyran crosses the Tanneron and Esterel massifs, while the Argens crosses the Permian depression before merging with the Reyran less than 400 m upstream of the river mouth. Bellaiche (1965) described the Quaternary sediments deposited in the Gulf of Fréjus after the Last Glacial Maximum, which constitute a conglomerate disappearing at a water depth of about 80–90 m corresponding to the late glacial coastline (Bellaiche, 1969a). The conglomerate is about 10 cm thick and is covered by terrigeneous transgressive deposits (Flandrian transgression). The late Holocene surface sediments are composed of a soft, dark-beige mud with high water content which thins towards the continental shelf edge (Bellaiche, 1965; Bellaiche et al., 1969). The shallowest extent of these late Holocene muds (mud-line of Bellaiche, 1969b) was located at a water depth of 15 m prior to the Malpasset Dam breakage (Nesteroff, 1965) and 23 m following the event (Bellaiche, 1969a). At water depths shallower than 15 m, the mud is replaced by coarse shoreface deposits (Bellaiche, 1969a). Seaward of the shelf break, the Argens–Reyran river system continues through the deep Fréjus canyon (Fig. 1).

2.1. The 1959 flood

The Malpasset Dam was a 60-m-high arch-dam built between 1951 and 1954, located 14 km upstream of the river mouth. On December

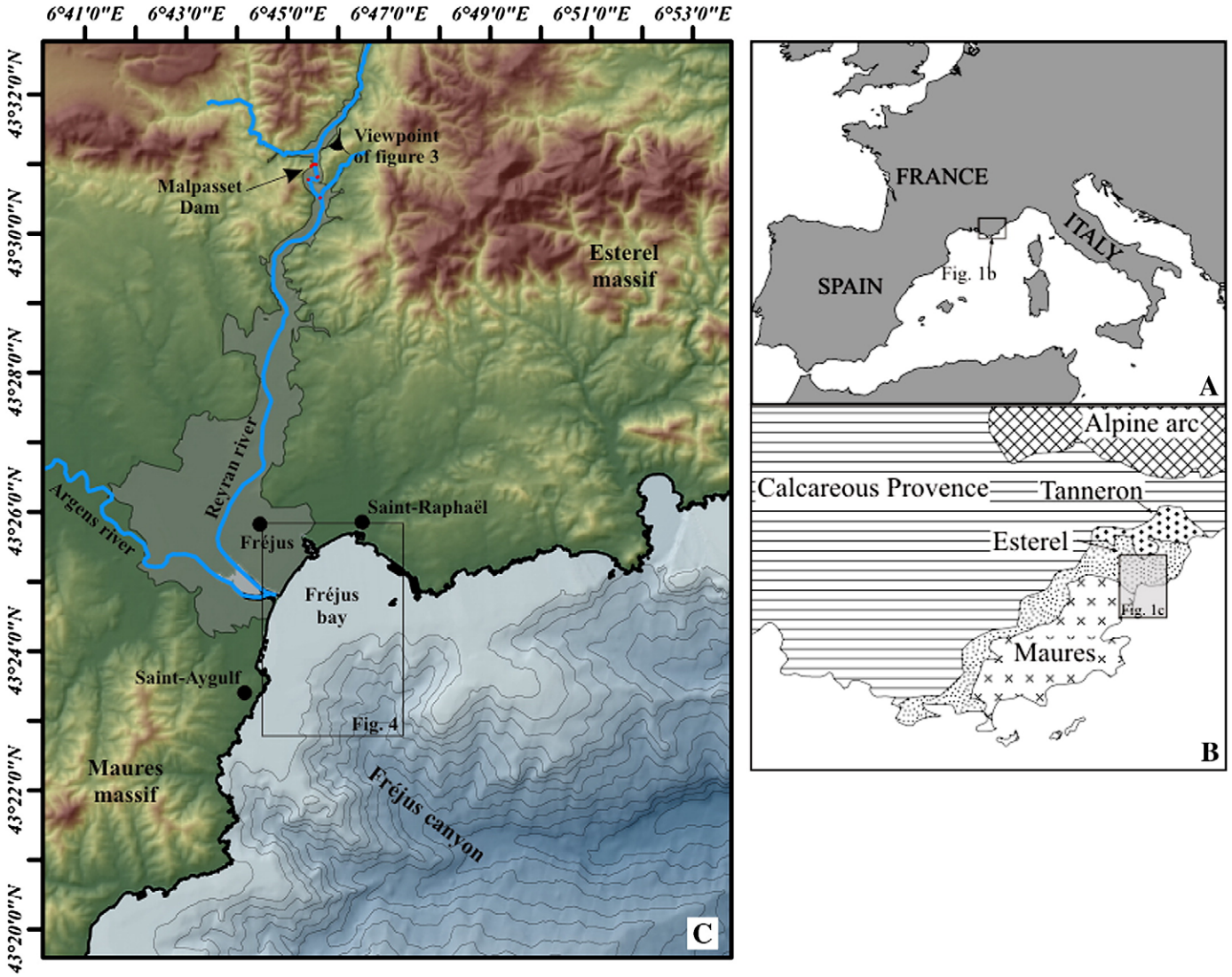

Fig. 1. Location map showing the study area, the Gulf of Fréjus, the Reyran and Argens rivers and the multibeam bathymetry of the Gulf of Fréjus and Fréjus Canyon. (Bathymetric map courtesy of B. Savoye, Ifremer data). A: Location of study area. B: Regional geology of Provence. C: Morphologic and bathymetric map of study area.

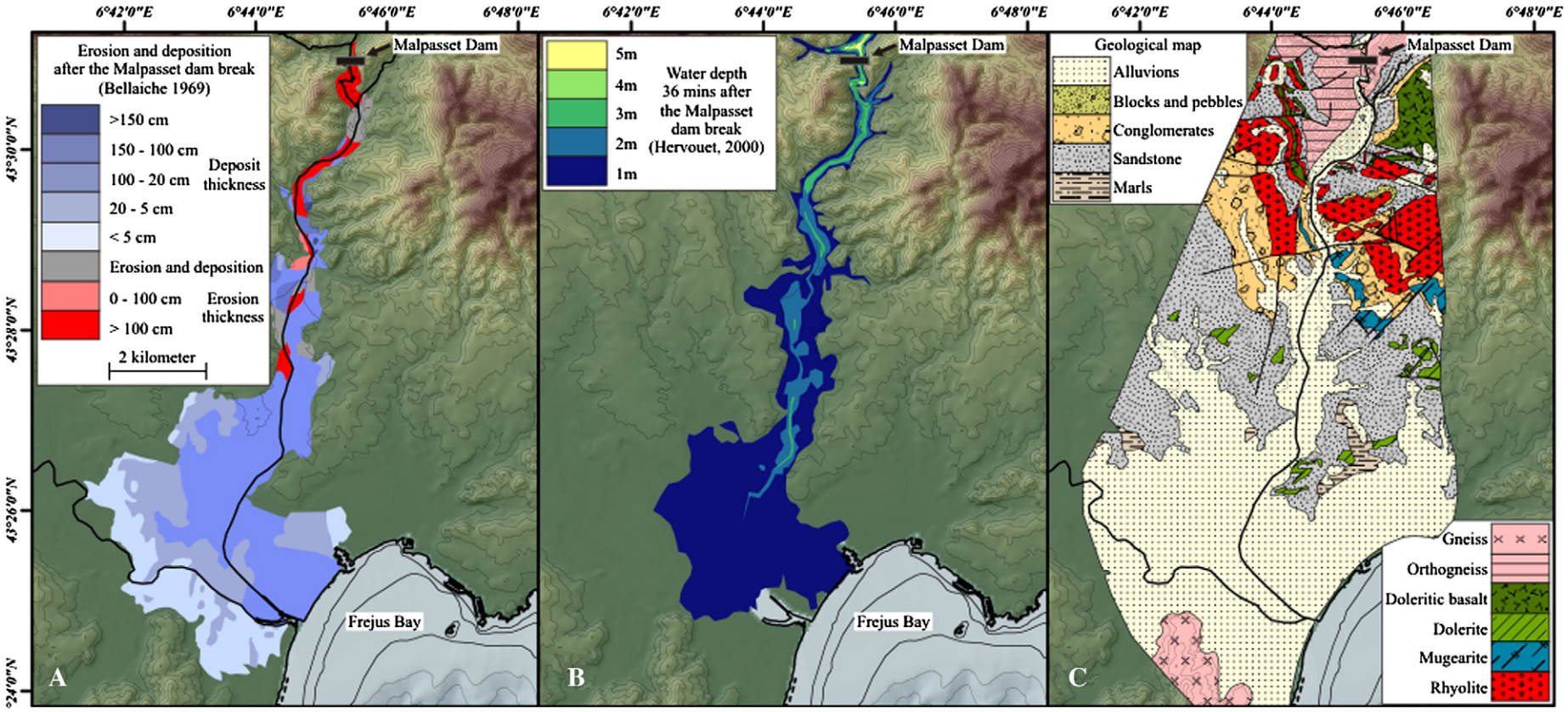

Fig. 2. A: Thickness of erosion and deposition on the continent between Malpasset dam and the city of Fréjus (from Bellaiche, 1965) after the 1959 event. B: Simulation of the wave created onland after the dam breaking (Hervouet, 2000). C: Simplified geological map across the drainage basin of Argens and Reyran rivers.

2nd, 1959, the Dam broke and discharged 49×10^6 m^3 of water into the lower Reyran valley at a velocity of up to 20 m s^{-1}. The maximum depth of erosion reached locally 10 m immediately downstream of the dam (Bellaiche, 1969a) and more than 5 m in the city of Fréjus as shown by the limits of urban destruction. Numerical modelling using the Telemac 2D model (Hervouet, 2000; Fig. 2B) suggests that the flood had a total duration of about 20 min. The event caused 439 casualties, mainly located in the city of Fréjus.

2.2. Subaerial deposits

Aerial photographs taken just after the catastrophe show that subaerial deposits formed a large sheet of silty to sandy mud that covered most of the city of Fréjus and surrounding areas (Fig. 3). These deposits have been mapped by Bellaiche (1969a; Fig. 2C). They cover a wide area beginning ~8 km (straight-line distance) from the coastline and represent an estimated volume of 4,515,400 m^3. The thickness of deposits varies from a few centimetres to more than 1.5 m (Fig. 2C). In many locations, erosion and sedimentation appear to have been simultaneous processes. In particular, soft coastal deposits (loose sand) were eroded and transported downstream in the Mediterranean Sea.

3. Data and methods

The data were collected during the Carma cruise (2001) on the N/O Tethys 2 using both a traditional Kullenberg corer and a Barnett interface gravity multi-corer (Barnett et al., 1984). 16 interface cores and 11 Küllenberg cores with lengths varying from 1.2 to 2.65 m were collected on the continental shelf and Fréjus Canyon (Fig. 4). These corings add to the database of 353, 1.5 m-long Kullenberg cores collected on the continental shelf by Bellaiche (1965). For the Carma cruise cores, a 1 cm-thick slab was sampled along each core and was X-radiographed using the Scopix system (Migeon et al., 1999) combining an X-ray imaging system and image analysis software. Grain size

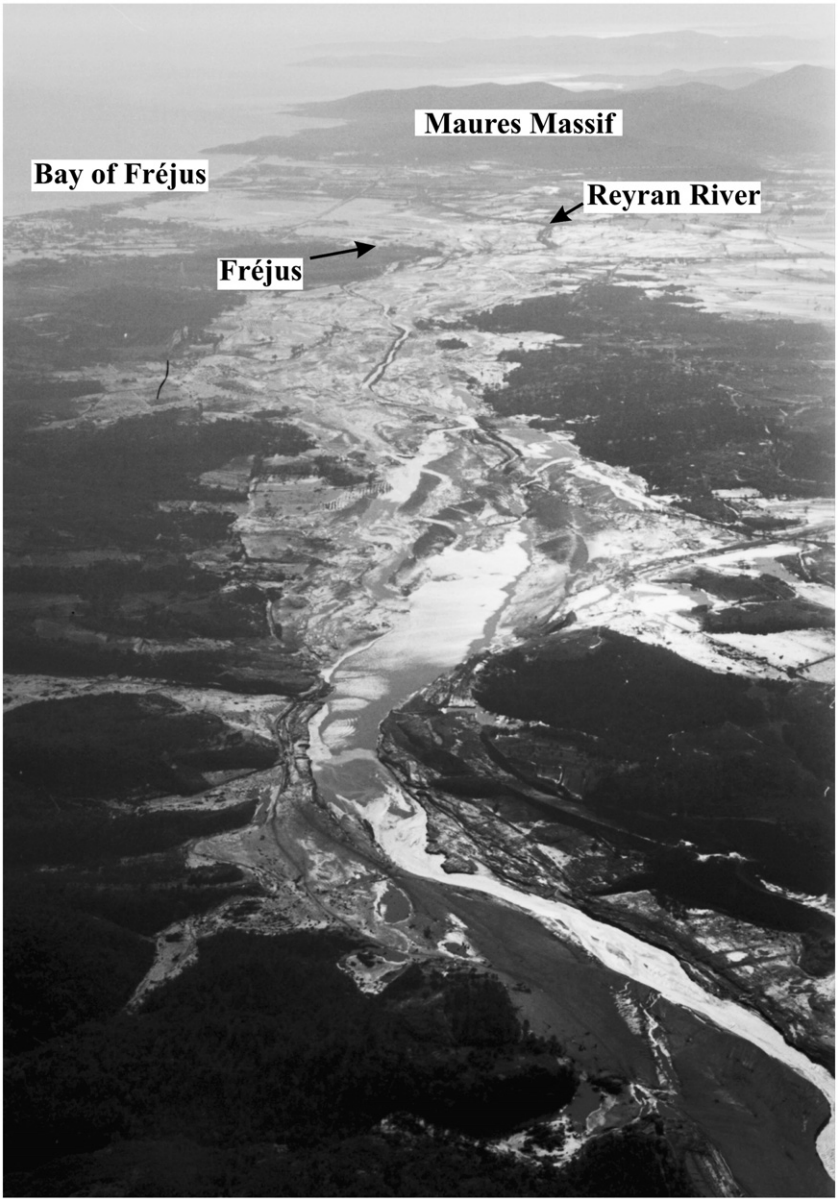

Fig. 3. Subaerial photograph published in the weekly paper "Paris Match" (no. 557, Saturday, December 12th, 1959; photographer: Gery) showing a good view of the area affected by the flood. The white tone corresponds to the extent of the deposits. The viewpoint is approximately from the Malpasset dam which is located just right of the right-hand bottom corner (see Fig. 1 for viewpoint location). The photograph is oriented towards the South. Reproduced by permission of Paris-Match.

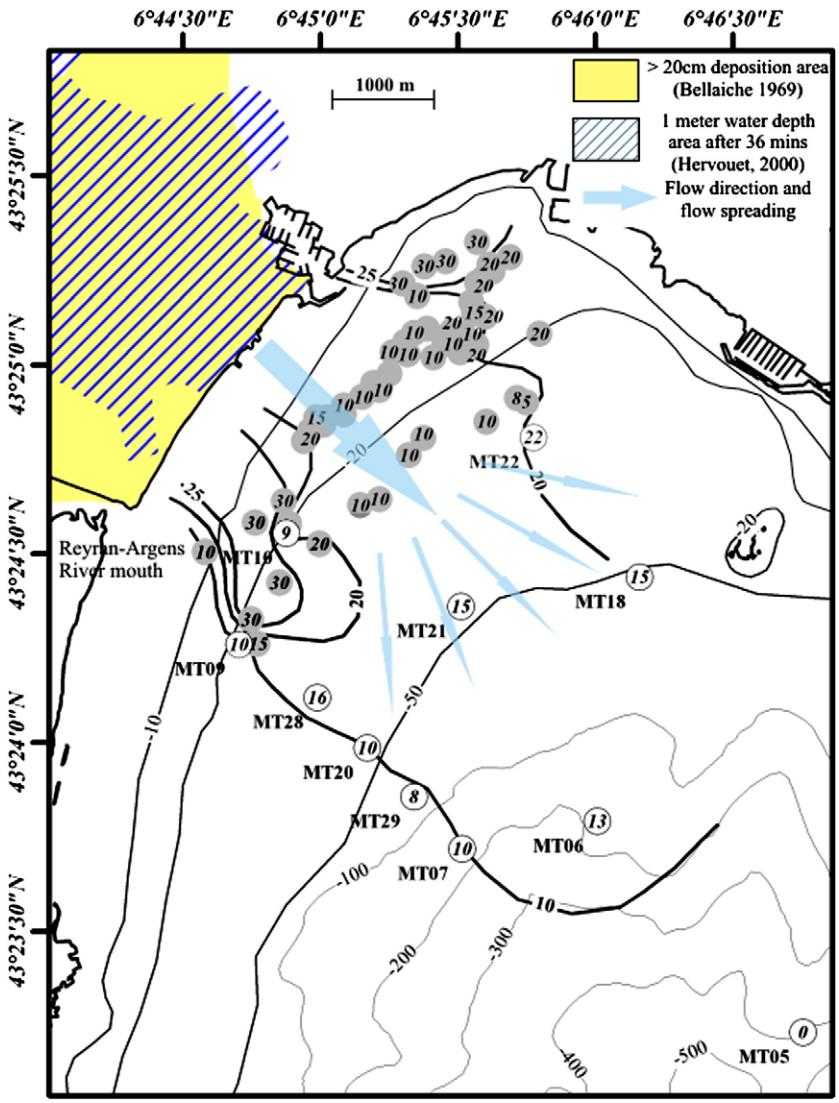

Fig. 4. Location of cores collected during the Carma cruise (2001, white circles) and cores from Bellaiche (1969a) in which the Malpasset dam break deposit has been observed. Values in the circles indicate the thickness of the deposits related to the Malpasset dam break. The solid black line represents the isopach map of these deposits. See Fig. 1 for location. Arrows indicate main axis of flow path when entering the sea and location of flow spreading and rapid freezing.

was measured using a laser diffractometer Malvern Mastersizer. In addition, large thin sections were made to aid interpretation.

Analysis of the detrital petrography was performed after sieving at 90 and 150 μm. The age of the most recent deposits was provided by counting the activity of radiogenic isotopes: ^{137}Cs (resulting from subaerial nuclear tests) and $^{210}Pb_{exc}$ (half-life = 22.4 yr) were counted over 20 h using a high-resolution gamma spectrometer with a semi-planar detector. $^{210}Pb_{exc}$ = total $^{210}Pb - ^{226}Ra$. No activity can be detected after a period corresponding to five to six times the half-life at the maximum (Jouanneau et al., 1988; Gouleau et al., 2000). The appearance of ^{137}Cs marks the beginning of nuclear tests in atmosphere (year 1952). The peak of ^{137}Cs corresponds to the most intense testing period (1963). In coarse deposits, sediments were sieved at 150 μm to concentrate the fine fraction. This method is appropriate in this study because we do not calculate sedimentation rates but simply need to verify the young age of the uppermost deposits in the cores.

4. Results

11 interface cores collected on the continental shelf during the Carma cruise and 48 cores from Bellaiche (1965) contain an organic-rich layer of 10–40 cm thickness (Fig. 5), deposited above olive-grey to dark olive-grey bioturbated mud (Fig. 5). This organic-rich layer is limited by a basal sharp or erosive surface and is dominated by coarse sand to silt grain sizes. The grain size analysis shows that the hemipelagic mud has a constant grain size (e.g. cores MT01, MT02, MT03 and MT05 in Fig. 6). This constant grain size allowed easy identification of the base of the Malpasset Dam deposits. For cores containing this deposit, grain size distributions show bimodal curves with peaks at 80 μm and 120 μm. The maximum grain size is about 45 μm for the d50 curve and between 160 and 245 μm for the d90 curve. All the cores containing this layer are located on the inner continental shelf between 6°44′30″E and 6°46′00″E and 43°25′30″N and 43°24′00″N. Most of these coarse deposits are located at water depths shallower than 23 m (Fig. 4).

Vertical grain size distribution (Fig. 6) shows either no grading or a crude coarsening-up trend, for example on MT 10 and 9. No sedimentary structure or bioturbation is visible in the dark layer. Binocular and thin section analysis show that the dark layer contains abundant quartz, mica, feldspar, pebble, rock fragments (essentially Permian pelites and gneiss), and frequent gastropods (Turritella) of 3–5 cm length. It contains also numerous vegetal remains (pine-cone

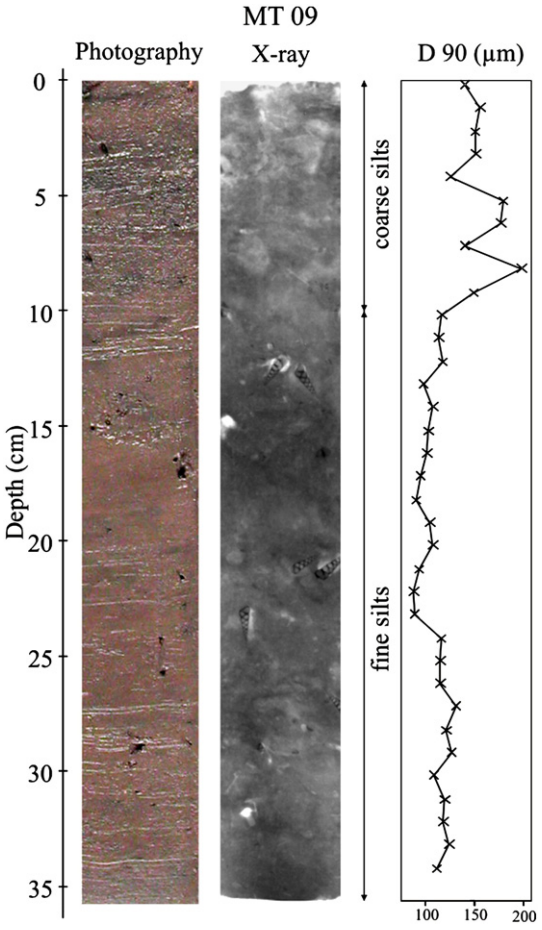

Fig. 5. Interface cores showing the sequence deposited by the Malpasset Dam failure in MT 9 photograph, X-ray (Scopix) image; grain size curve (d90 values).

fragments, leaves) and humans artefacts (peach stone, plastic fragments). Bellaiche (1965) showed that the heavy mineral suite is essentially composed of amphiboles, staurolite, disthenes, andalousite, garnets, tourmaline, zircon and monoclinic pyroxene.

$^{210}Pb_{exc}$ and ^{137}Cs show activity varying from a few Bq/kg to 100 Bq/kg at the base of the hemipelagic beige sediment overlying the dark deposits.

The spatial extent of our cores is larger than the set of Bellaiche (1965, 1969a) and permits the development of a more accurate isopach map of this layer (Fig. 4). This map suggests that the dark sandy surface layer effectively thins seaward but that the deposit thickness also varies along a transversal cross section. Deposits are thicker (up to 30 cm) on both sides of the location where the flow entered the sea, just north of the present Reyran river mouth, and thinner in the axis of the flow path (Fig. 4).

5. Discussion

Eight lines of evidence suggest that the thin (less than 30-cm thick), dark, sandy-silt layer can be interpreted as deposits resulting from the failure of the Malpasset Dam. (1) The deposits are of terrigeneous origin as suggested by the presence of coarse particles, pebbles, vegetal fragments or anthropogenic material. Their distribution over a very small area of the inner continental shelf at the mouth of the Reyran–Argens rivers is also consistent with a terrigeneous source. (2) The submarine deposits are a continuous extension of those deposited on land by the flood. (3) These deposits were not described in studies of the surface deposits previous to the 1959 event (Nesteroff, 1965; Bellaiche, 1969a). (4) This dark layer lies on the beige mud interpreted as late Holocene deposits by Bellaiche (1969b). (5) These recent deposits form a seaward-prograding wedge with thickness decreasing from 30 to 0 cm. Nesteroff (1965) showed that the shallowest extent of the late Holocene mud was close to isobath 15 m. Bellaiche (1965) suggests that the shallowest extent of the mud line after the dam break was located between isobaths −20 and −23 m. Our new data show that the deposits related to the dam break extend slightly deeper than isobath 30 m. However, at a water depth deeper than 20–25 m, the dark layer is thin and probably discontinuous (Bellaiche did not detect it in cores) suggesting that the flow spread at this location. These results suggest that the dark layer covered the older Holocene mud, leading to the deepening of the mud line. (6) The presence of a sharp or erosive basal surface suggests an energetic process for the deposition of this dark layer. (7) The grain-size of the deposits is very similar to the grain size of the deposits deposited onland after the dam broke (Bellaiche, 1969a). (8) The $^{210}Pb_{exc}$ and ^{137}Cs dating show that the dark sandy-silt layer is covered with centimetre-thick mud drape with an age of <100 years.

The analysis of the detrital petrography shows that the origin of the deposit is the Tanneron massif (gneiss) and the Permian depression (red Permian clasts). Abundance of quartz, mica and feldspar is characteristic of the rocks surrounding the dam and deposited in the Reyran River. The heavy minerals are typical both of the Argens River and the Fréjus beach. Only the zircon and the monoclinic pyroxenes suggest a source from the Reyran River (Bellaiche, 1969a). This is explained by the fact that Argens and Reyran rivers merge 400 m upstream of the river mouth and that a large part of the Fréjus beach sand was reworked and transported downstream during the flood, as shown on the subaerial photograph (Fig. 2). This erosion of Fréjus beach is also consistent with the two peaks in the grain-size distribution curve.

The transversal and longitudinal variations in deposit thickness are very informative regarding the flow behaviour. The thicker deposits observed on both sides of the point where the flow entered the sea suggest that the flow behaved as a typical planar jet flow of Bates (1953) or inertia-dominated flow of Wright (1977). The quick thinning and disappearing of the deposits seaward (in less than 4 km) is consistent with such a behaviour. This behaviour is typical of a fast-moving, high-concentration, bedload-dominated flow. The shear resistance is higher on the sides of the flow, where freezing occurs more rapidly and more intensely, generating coarse deposits with a levee shape while the flow continues to bypass along the main axis of transport where the driving force exceeds the shear resistance (Fig. 4). This kind of deposit has been described in friction-dominated (hyperconcentrated flow and debris flow deposits) both in subaerial (Johnson, 1970, 1984) and submarine (Middleton and Hampton, 1973) environments.

These results suggest that the coarse, dark deposit observed in cores was generated by the violent flood caused by the Malpasset Dam failure, and, in that sense, they correspond to a fast hyperpycnal flow. However, the deposits do not show the classical coarsening and fining-up intervals described by Mulder et al. (2003) in hyperpycnites. The explanation probably relates to the nature, magnitude and brief duration of the processes. The 1959 flood corresponds to a typical surge-like flood. This means that the peak discharge occurred suddenly without any preliminary period of increasing discharge (the waxing flow of Kneller, 1995; Kneller and Branney, 1995). In addition, the energy of the surge suggested by the height of the flood wave generated erosion before rapid deposition. Deposits on the continent have a sheet-like shape suggesting that the flow behaved as a hyperconcentrated flow (inertia flow) with deposition occurring through freezing ("en masse" deposition; Middleton and Hampton, 1973; Lowe, 1979, 1982). Deposition was thus too fast to generate any sedimentary structure. The rapid freezing was probably intensified

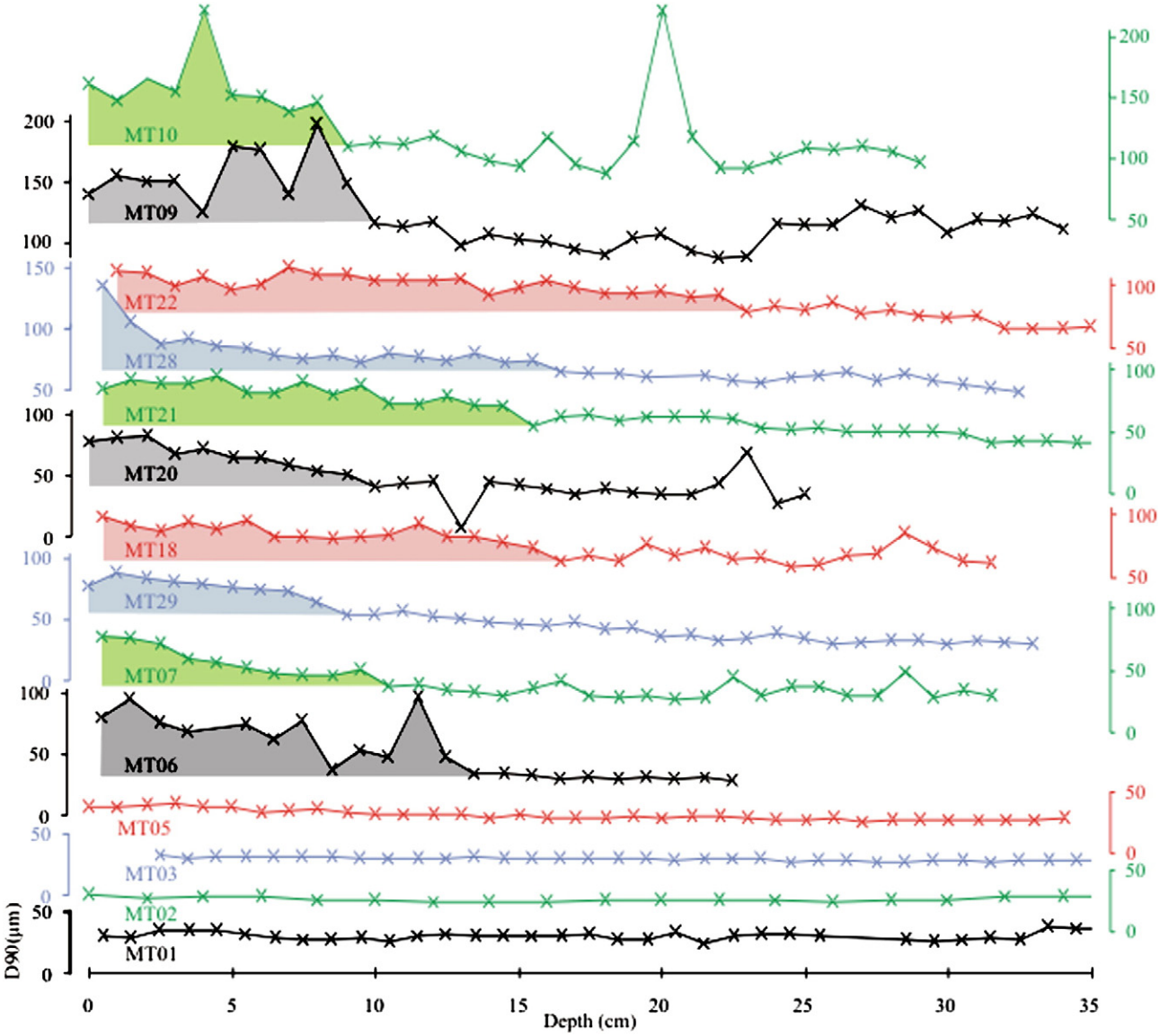

Fig. 6. Synthesis of grain size analysis on Carma cruise cores (d90 values). The hemipelagic limit (approximately 50 µm) is used to delimitate the base of the Malpasset deposits that are figures in colour.

when flow spread, at a water depth of 20–25 m, i.e. at the location where Bellaiche (1969a) identified the post-event mudline. The continuity between subaerial and submarine deposits suggests that the process did not drastically change when the flow entered the sea. No grading is visible in the dark layer in cores MT9 and MT10 suggesting that no preferential fallout of particles occurred during deposition. This is consistent with the presence of a progradational wedge of sand deposited above the hemipelagic mud as described by Bellaiche (1969a; Fig. 7). The deposits are similar to the massive sand beds described by Zuffa et al. (2000) related to the Missoula Lake floods. However, these authors also described thinner beds with a crude grading corresponding to the Ta interval of the Bouma sequence (Bouma, 1962) or the concentrated flow deposits of Mulder and Alexander (2001). The lack of grading in the Malpasset Dam deposits can be explained by the small magnitude of the event when compared to the Lake Missoula events. Freezing of the flow was too fast to permit any differentiation at the upper flow interface. Another difference with deep-sea hyperpycnites (Mulder et al., 2001a, 2002) is the restricted extent of the deposits to the inner continental shelf. None of the cores collected in the Fréjus Canyon show recent deposits. Four explanations can be provided for this point: (1) the coarse particle sizes of the sediment deposited in the Reyran and Argens rivers and transported during the flood. Most of the coarse particles come from Hercynian and Permian crystalline massifs, and are composed of rock clasts and dense quartz, micas and feldspar with a grain-size ranging between sand and medium silts. This suggests that these particles were transported as bedload rather than suspended load. (2) The short duration of the event. A surge like flood lasts only a few minutes, and is typically unsteady, first instantaneously waxing, and then quickly waning. This kind of behaviour does not allow bedload transport over a long distance. To be transported over long distances, coarse particles require events of long duration and sustained intensity. (3) As shown by aerial photographs and sediment analysis onland (Bellaiche, 1965), a large amount of the sediments transported during the flood were deposited on the continent. Only a small part of the particles eroded in the Reyran valley were transported into the marine environment. Most of the submarine deposits come from erosion downstream of the Reyran–Argens junction and from erosion

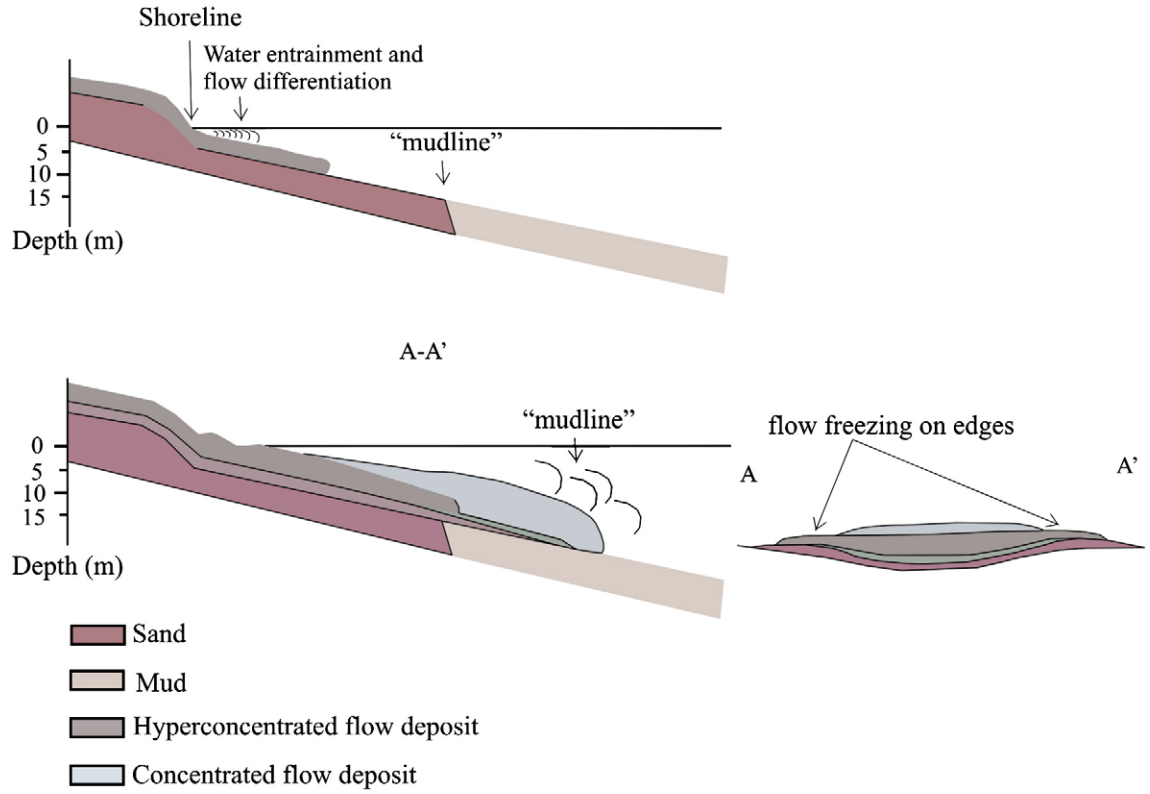

Fig. 7. Schematic interpretation of the flow process in the case of a bedload-dominated hyperpycnal flow. This model integrates data from the Malpasset dam (this study) and Missoula Lake flood deposits (Zuffa et al., 2000). The hyperconcentrated flow enters the see and freezes rapidly leading to the "mudline" progradation (Malpasset event). The faster freezing on flow sides forms crude levee-shape deposits. If the event is large enough, flow differentiation can occur at the upper part of the flow and a concentrated flow forms depositing a Ta interval with a crude grading (Missoula lake flood deposits). This transformation was not observed in the Malpasset Dam break-related flood because the magnitude of the flash flood was too small.

of sand on the Fréjus Beach. (4) The fast spreading and freezing of the flow.

6. Conclusions

The Malpasset Dam failure provides a good example of a surge-like hyperpycnal flow. When entering the sea, its behaviour provides a typical example of an inertia-dominated flow. The deposits related to this sudden flooding event can be found both on land and at sea. In the marine environment, the main deposits are restricted to a narrow and shallow strip between the shoreface and −23 m isobath. Deposits extend more sparsely down to isobath −30 m. An organic-rich, fining-up sandy-silt layer of a few decimetres thickness that prograded over the late Holocene mud constitutes the flood-related deposits. The detrital petrography clearly indicate a source from the Reyran and Argens rivers and erosion of the beach of Fréjus.

The deposits associated with the Malpasset Dam failure strongly differ from classical hyperpycnites because:

- The process relates to an intense, unsteady surge-flow of short duration, very different from the steady flow sustained over days to weeks during a seasonal river flood;
- Suspended load is very low; the flow is essentially bedload-dominated.

Consequently, the process is closer to a slide-triggered, surge-like flow forming a hyperconcentrated flow, with the only difference being the presence of fresh water in the Malpasset surge and salt–water in a slide-triggered turbidity current. The Malpasset flood deposit is a good analogue for surge-like floods generated by the breaking of natural dams, such as those producing jökulhlaups, or deposits resulting from sudden discharge of subglacial lakes during deglaciation because:

- Most of the floods in these subglacial environments result from the rapid draining of a reservoir, usually a fresh-water subglacial lake;
- The nature of eroded particulate material (volcanic rock in Iceland, moraine deposits on a glaciated margin) generates primarily coarse particles prone to bedload transport.

Acknowledgements

The authors thank the crew and the Captain of the *Tethys II* during the Carma cruise. We thank Bruno Savoye for providing multibeam bathymetric map of the Gulf of Fréjus. The authors are very grateful to Takeshi Nakajima and an anonymous reviewer for their valuable comments on the manuscript and to William Fletcher for the reading of the paper for final English polishing. This represents UMR CNRS 5805 EPOC contribution 1727.

References

Baker, V.R., Bunker, R.C., 1985. Cataclysmic late Pleistocene flooding from glacial Lake Missoula; a review. Quat. Sci. Rev. 4, 1–41.
Barnett, P.R.O., Watson, J., Connelly, D., 1984. A multiple corer for taking virtually undisturbed samples from shelf, bathyal and abyssal sediments. Oceanol. Acta 7, 399–408.
Bates, C.C., 1953. Rational theory of delta formation. Bull. Am. Ass. Petrol. Geol. 37 (9), 2119–2162.
Bellaiche, G., 1965. Contribution à l'étude de la sédimentation actuelle dans le Golfe de Fréjus. Thèse 3ème cycle, Paris,
Bellaiche, G., 1969a. Etude géodynamique de la marge continentale au large du massif des Maures (Var) et de la plaine abyssale ligure. Thèse d'état, Univ. Paris, 221 pp.
Bellaiche, G., 1969b. Les dépôts Quaternaires immergés du golfe de Fréjus (Var) France. Part 4. Coastal and shallow water sedimentation: eustatic and tectonic effects, pp. 171–176.

Bellaiche, G., Vergnaud-Grazzini, C., Glangeaud, L., 1969. Les épisodes de la transgression flandrienne dan le Golfe de Fréjus. C. R. Acad. Sci., Paris 268 (série D), 2765–2770.
Bouma, A.H., 1962. Sedimentology of Some Flysch Deposits: A Graphic Approach to Facies Interpretation. Elsevier, Amsterdam. 168 pp.
Brunner, C.A., Normark, W.R., Zuffa, G.G., Serra, F., 1999. Deep-sea sedimentary record of the late Wisconsin cataclysmic floods from the Columbia River. Geology 27 (5), 463–466.
Dromart, G., Quantin, C., Broucke, O., 2007. Stratigraphic architectures spotted in southern Melas Chasma, Valles Marineris. Mar. Geol. 35 (4), 363–366.
Einarsson, P., Brandsdóttir, B., Tumi Gudmunsson, M., Björnsson, H., Grönvold, K., Sigmundsson, F., 1997. Center of the Iceland hotspot experiences volcanic unrest. Eos, Trans. Am. Geophys. Union 78 (35), 369–375.
Gouleau, D., Jouanneau, J.-M., Weber, O., Sauriau, P.G., 2000. Short term, long term sedimentation on Montportail–Brouage intertidal mudflat, Western side of Marennes Oléron Bay (France). Cont. Shelf Res. 20, 1513–1530.
Gilbert, G.K., 1878. The ancient outlet of Great Salt Lake. Am. Jour. Sci., 3rd Series 15, 256–259.
Grönvold, K., Jóhannesson, H., 1984. Eruption in Grímsvötn 1983, course of events and chemical studies of the tephra. Jökul 34, 1–11.
Gudmunsson, M.T., Sigmundsson, F., Björnsson, H., 1997. Ice-volcano interaction of the 1996 Gjálp subglacial eruption, Vatnajökull, Iceland. Nature 389, 954–957.
Hervouet, J.-M., 2000. A high resolution 2-D dam-break model using parallelization. Hydrol. Process. 14, 2211–2230.
Johnson, A.M., 1970. Physical Processes in Geology. Freeman, Cooper and Co., San Francisco. 577 pp.
Johnson, A.M., 1984. Debris flow. In: Brunden, D., Prior, D.B. (Eds.), Slope Instability. Wiley, Toronto, pp. 257–362.
Jouanneau, J.-M., Garcia, C., Oliveira, A., Rodrigues, A., Dias, J.A., Weber, O., 1988. Dispersal and deposition of suspended sediment on the shelf off the Tagus and Sado estuaries, SW Portugal. Prog. Oceanogr. 42 (1–4), 233–257.
Kneller, B.C., 1995. Beyond the turbidite paradigm: physical models for deposition of turbidites and their implications for reservoir prediction. In: Hartley, A.J., Prosser, D.J. (Eds.), Characterization of Deep Marine Clastic Systems. Spec. Publ., vol. 94. Geol. Soc. London, pp. 31–49.
Kneller, B.C., Branney, M.J., 1995. Sustained high-density turbidity currents and the deposition of thick massive beds. Sedimentology 42, 607–616.
Lowe, D.R., 1979. Sediment gravity flows: their classification and some problems of application to natural flows and deposits. In: Doyle, N.J., Pilkey, O.H. (Eds.), Geology of Continental Slopes. Soc. Econ. Paleont. Mineral. Spec. Publ., vol. 27. Tulsa, pp. 75–82.
Lowe, D.R., 1982. Sediment gravity flows: II. Depositional models with special reference to the deposits of high-density turbidity currents. J. Sed. Petrol., 52, 279–297.
Malde, H.E., 1968. The Catastrophic Late Pleistocene Bonneville Flood in the Snake River Plain, Idaho. Geol. Survey Prof. Paper, vol. 596. U. S. Government Printing Office, Washington. 69 pp.
Malde, H.E., Powers, H.A., 1962. Upper Cenozoic stratigraphy of the western Snake River plain, Idaho. Geol. Soc. Am. Bull. 73 (10), 1197–1219.
Middleton, G.V., Hampton, M.A., 1973. Sediment gravity flows: mechanics of flow and deposition. In: Middleton, G.V., Bouma, A.H. (Eds.), Turbidity and Deep Water Sedimentation, Soc. Econ. Paleont. Mineral., Pacific Section, Short Course Lecture Notes, pp. 1–38.
Migeon, S., Weber, O., Faugères, J.-C., Saint-Paul, J., 1999. SCOPIX: a new X-ray imaging system for core analysis. Geo-Mar. Lett. 18, 251–255.
Milliman, J.D., Syvitski, J.P.M., 1992. Geomorphic/tectonic control of sediment discharge to the ocean: the importance of small mountainous rivers. J. Geol. 100, 525–544.
Milliman, J.D., Kao, S.-J., 2005. Hyperpycnal discharge of fluvial sediment to the ocean: impact of Super-Typhoon Herb (1996) on Taiwanese rivers. J. Geol. 113, 503–516.
Mullineaux, D.R., Wilcox, R.E., Ebauch, W.F., Fryxell, R., Rubin, M., 1978. Age of the last major Scalbland flood of the Columbia Plateau in eastern Washington. Quat. Res. 10, 171–180.
Mulder, T., Syvitski, J.P.M., 1995. Turbidity currents generated at river mouths during exceptional discharges to the world oceans. J. Geol. 103, 285–299.
Mulder, T., Alexander, J., 2001. The physical character of sedimentary density currents and their deposits. Sedimentology 48, 269–299.
Mulder, T., Savoye, B., Piper, D.J.W., Syvitski, J.P.M., 1998a. The Var submarine sedimentary system: understanding Holocene sediment delivery processes and their importance to the geological record. In: Stocker, M.S., Evans, D., Cramp, A. (Eds.), Geological Processes on Continental Margins: Sedimentation, Mass-wasting and Stability. Spec. Publ., vol. 129. Geol. Soc., London, pp. 145–166.
Mulder, T., Syvitski, J.P.M., Skene, K.I., 1998b. Modelling of erosion and deposition by turbidity currents generated at river mouths. J. Sed. Res. 68, 124–137.
Mulder, T., Migeon, S., Savoye, B., Faugères, J.-C., 2001a. Inversely-graded turbidite sequences in the deep Mediterranean. A record of deposits from flood-generated turbidity currents? Geo-Mar. Lett. 21, 86–93.
Mulder, T., Migeon, S., Savoye, B., Jouanneau, J.-M., 2001b. Twentieth century floods recorded in the deep Mediterranean sediments. Geology 29 (11), 1011–1014.
Mulder, T., Migeon, S., Savoye, B., Faugères, J.-C., 2002. Inversely-graded turbidite sequences in the deep Mediterranean. A record of deposits from flood-generated turbidity currents? A reply. Geo-Mar. Lett. 22 (2), 112–120.
Mulder, T., Syvitski, J.P.M., Migeon, S., Faugères, J.-C., Savoye, B., 2003. Hyperpycnal turbidity currents: initiation, behavior and related deposits. A review. In: Mutti, E., Steffens, G.S., Pirmez, C., Orlando, M., Roberts, D. (Eds.), Turbidites: Models and Problem, pp. 861–882.
Nakajima, T., 2006. Hyperpycnites deposited 700 km away from river mouths in the central Japan Sea. J. Sedim. Res. 76, 60–73. doi:10.2110/jsr.2006.13.
Nesteroff, W.D., 1965. Recherches sur les sédiments marins actuels de la région d′ Antibes. Ann. Inst. Océanogr. 43 (Fasc. 1) 136pp..
Normark, W.R., Piper, D.J.W., 1991. Initiation processes and flow evolution of turbidity currents: Implications for the depositional record. In: Osborne, R.H. (Ed.), From Shoreline to Abyss; Contribution in Marine Geology in Honor of Francis Parker Shepard, SEPM, Spec. Publ. 46, Tulsa, pp. 207–230.
Richmond, G.M., Fryxell, R., Neff, G.E., Trimble, D.E., 1965. The Cordilleran Ice Sheet of the northern Rocky Mountains, and related history of the Columbia Plateau. In: Wright, H.B., Frey, D.G. (Eds.), The Quaternary of the United States. Princeton Univ. Press, Princeton, pp. 231–242.
Saint-Onge, G., Mulder, T., Piper, D.J.W., Hillaire-Marcel, C., Stoner, J., 2003. Earthquake and flood-induced turbidites in the Saguenay Fjord (Québec): a Holocene paleoseismicity record. Quat. Sci. Rev. 23, 283–294.
Shipboard Scientific Party, 1998a. Introduction. In: Fouquet, Y., Zierenberg, R.A., Miller, D.J. (Eds.), Proc. ODP. Init. Repts., vol. 169. Ocean Drilling Program, College Station, TX, pp. 7–16. doi:10.2973/odp.proc.ir.169.101.1998.
Shipboard Scientific Party, 1998b. Escanaba Trough: reference site (Site 1037). In: Fouquet, Y., Zierenberg, R.A., Miller, D.J. (Eds.), Proc. ODP. Init. Repts., vol. 169. Ocean Drilling Program, College Station, TX, pp. 205–251. doi:10.2973/odp.proc.ir.169.105.1998.
Shipboard Scientific Party, 1998c. Escanaba Trough: Central Hill (Site 1038). In: Fouquet, Y., Zierenberg, R.A., Miller, D.J. (Eds.), Proc. ODP. Init. Repts., vol. 169. Ocean Drilling Program, College Station, TX, pp. 253–298. doi:10.2973/odp.proc.ir.169.106.1998.
Waitt, R.B., 1985. Case for periodic, colossal jökulhlaups from Pleistocene glacial Lake Missoula. Geol. Soc. of Am. Bull. 96, 1271–1286.
Warrick, J.A., Milliman, J.D., 2003. Hyperpycnal sediment discharge from semiarid southern California rivers: implications for coastal sediment budgets. Geology 31 (9), 781–784. doi:10.1130/G19671.1.
Wright, L.D., 1977. Sediment transport and deposition at river mouths: a synthesis. Geol. Soc. Am. Bull. 88, 857–868.
Wright, L.D., Yang, Z.-S., Bornhold, B.D., Keller, G.H., Prior, D.B., Wisenam Jr., W.J., 1986. Hyperpycnal flows and flow fronts over the Huanghe (Yellow River) delta front. Geo-Mar. Lett. 6, 97–105.
Yu, H.-S., 2006. Hyperpycnal discharge of fluvial sediment to the ocean: impact of Super-Typhoon Herb (1996) on Taiwanese rivers: a discussion. J. Geol. 114, 763–765.
Zierenberg, R.A., Fouquet, Y., Miller, D.J., Normark, W.R. (Eds.), 2000. Proc. ODP. Sci. Results, vol. 169. Ocean Drilling Program, College Station, TX. doi:10.2973/odp.proc.sr.169.2000.
Zuffa, G.G., Normark, W.R., Serra, F., Brunner, C.A., 2000. Turbidite megabeds in an oceanic rift valley recording jökulhlaups of Late Pleistocene Glacial Lakes of the Western United States. The Journal of Geology 108, 253–274.